Preparation of Mechanical Alloying AlCuFe Alloy and Its Application in Li-Ion Battery Anode

Xiao Lan, Zhanhao Sun and Xunyong Jiang

Abstract Aluminum has high lithium storage capacity and poor cycle performance as one kind of new advanced material. In this paper, $Al_{64}Cu_{23.5}Fe_{12.5}$ alloy was prepared by mechanical alloying with pure Al, Cu, and Fe powder as the initial materials and the electrochemical lithium storage performance of AlCuFe ternary alloy was studied. The effects of different milling device and experimental parameters on the microstructure of the alloy were also studied. Magnetic measurement was performed on alloy under different MA state. The results of XRD show that the peak of the elemental phase widens with the increase of the grinding time. New phase appears at about 75 h. It is found that the magnetism of the alloy is weakened with the formation of the new alloy. The discharge capacity of AlCuFe increase with longer milling time. After a long milling time of 100 h in 500 rmp, $Al_{64}Cu_{23.5}Fe_{12.5}$ alloy exhibites the highest first discharge capacities of 314 mAh g^{-1}. Then the capacity gradually decays in the first 20 cycles and stabilizes at a range of 175–200 mAh g^{-1}, which corresponds to 68% of initial capacity. Compared with pure Al, AlCuFe alloy-show better cycle stability, this facile MA approach provides helpful synergistic effects.

Keywords Lithium ion battery · Anode material · Mechanical alloying AlCuFe

X. Lan · Z. Sun · X. Jiang (✉)
School of Materials Science and Engineering, Tianjin University of Technology, Tianjin, China
e-mail: jiangxunyong@tjut.edu.cn

X. Lan
e-mail: lanmiaosx@163.com

Z. Sun
e-mail: sunzhh_977@163.com

Y. Han (ed.), *Advances in Energy and Environmental Materials*,
Springer Proceedings in Energy, https://doi.org/10.1007/978-981-13-0158-2_3

Introduction

An increasing number of electric or plug-in hybrid vehicles, portable electronic devices, and power tool technologies require a significant increase of the energy density of Li-ion batteries [1]. As a result of small size, high capacity and long cycle life advantages, lithium-ion batteries are increasingly widely used in all aspects of life, such as mobile phones, computers and other electronic products [2]. Currently, commercial LIB technology generally employs synthetic graphite as an anode for LIB batteries due to its stable cycling performance. However, critical problems such as limited raw material resources, complicated synthetic process, and high-temperature synthesis is still unresolved, leading to high synthetic graphite production costs. In addition, another issue of carbon materials is their low theoretical specific capacity of 372 mAh g^{-1}, leading to poor energy storage performance [3]. Therefore, to improve the capacity of LIB, anode with high theoretical capacity should be used, such as metal-based materials. Aluminum has high lithium storage capacity. However, these material always suffer rapid capacity fading arising from structural degradation and electrical contact loss during cycling. Aluminum-based intermetallic compounds can improve the cycling performance of Al anode through reducing the volume change of electrode by adding inert element into Al substrate, such as AlCuFe,which preventing the severe volume expansion stress of metal-based materials [4, 5]. Generally, AlCuFe alloy was prepared by melting and casting method. When the battery is assembled, it is also necessary to grind the casting alloy into powder. The mechanical alloying method (MA) can use elemental powder as the raw material to obtain the alloy powder. Mitka and Wang successfully prepared AlCuFe alloy using mechanical alloying process [6, 7]. In this paper, $Al_{64}Cu_{23.5}Fe_{12.5}$ was prepared by mechanical alloying using pure Al, Cu and Fe powder as the starting materials. The influence of the milling conditions on the phase structure of the alloy was studied. The electrochemical storage performance of AlCuFe alloy was measured.

Experimental

Elemental powders (99.9 wt% purity, average particle size in the range of 8–55 μm) of Al, Cu and Fe were mechanically alloyed to prepare the $Al_{64}Cu_{23.5}Fe_{12.5}$ element. The milling experiments were performed in a planetary ball mill (RE-QM-2SP12) and a high-energy vibrating ball mill (MSK-SFM-3). A 100 ml stainless steel vial and 3–10 mm (in diameter) stainless steel balls were used. The powders were balanced to give the nominal composition of $Al_{64}Cu_{23.5}Fe_{12.5}$ (at.%) and mixed in a glove box under a purified Ar atmosphere. The mixed powders were then sealed into the stainless steel vial. The ball to powder weight ratio was maintained as 20:1. N-hexane is surfactant to prevent welding of powder on the wall of mill pot. Argon is filled in mill to prevent powder and oxidation. Magnetic

measurements were made using VSM magnetic performance meter. Electrochemical measurements were performed using coin cells (CR2032, Hohsen Corporation), which are consist of $Al_{64}Cu_{23.5}Fe_{12.5}$ as the anode, Li metal foil (Honjo Chemical, 99.8%) as the cathode, a 1.0 M LiPF6 solution in a mixture of ethylene carbonateedimethyl carbonate (1:1) as the electrolyte, and a porous polypropylene membrane (Celgard 2400) as the separator. The $Al_{64}Cu_{23.5}Fe_{12.5}$ electrodes were prepared on a Cu foil substrate (Nippon Foil, 18 μm) as the current collector using coating an-methyl-2-pyrrolidinone solvent (NMP, Aldrich) based slurry with a mixture of 80 wt% of active materials, 10 wt% PVDF as the binder, and 10 wt% acetylene black as the conducting material. The resultant electrodes were dried in an oven at 90 °C for 9 h. All coin cells were assembled in a high-purity argon-filled glove box with H_2O and O_2 contents less than 5 ppm. The discharge-charge tests carried out using a battery cycler system (WonATech Corp., WMPG 3000) in the potential range of 0.0–2.0 V (vs. Li/Li þ) at 25 °C in an incubator. The cycling stability was observed up to 100 cycles at a current density of 100 mAh g^{-1}. XRD was carried out using the D/Max2500pc Rigaku/Japan instruments with Cu Kα radiation, the scan scope was set from 10° to 90°.

Results and Discussion

Experimental parameters of MA process. In this paper, MA were performed with planetary ball mill (RE-QM-2SP12) and high-energy vibrating ball mill (MSK-SFM-3). The influence of different mill appraptus on the phase evolusion during MA process was studied, as shown in Fig. 1. Figure 1a is the XRD results of AlCuFe power prepared by planetary ball milling and high energy vibration ball milling. As grinding time increases, the diffraction peak tends to widen significantly, indicating that the particle size decreases gradually with time. But before and after the curve in addition to the peak and no other changes, indicating that in this process there is no new phase of the formation. We speculate that the reason why no quasicrystal is generated is that the energy during the reaction is not enough, and then the change in the reaction process can be observed by increasing the milling time and the rotation speed.. MA process of high-energy vibrating ball mill is faster than planetary ball mill, Compared with high-energy vibration ball milling, the planetary ball mill can simultaneously mill four sets of samples, high-energy vibration ball milling can only mill a group of samples. So we chose the planetary ball milling in the following the experiment.

The reason of incomplete alloying of $Al_{64}Cu_{23.5}Fe_{12.5}$ may come from in sufficient energy in the milling process. The rotation speed should be get a higher level. Figure 1b is the XRD results of $Al_{64}Cu_{23.5}Fe_{12.5}$ powders under different rotation speed. It can be see that the diffraction peak widened with 550 rmp compared with 500 rmp, which indicates the grain refinement. High speed can

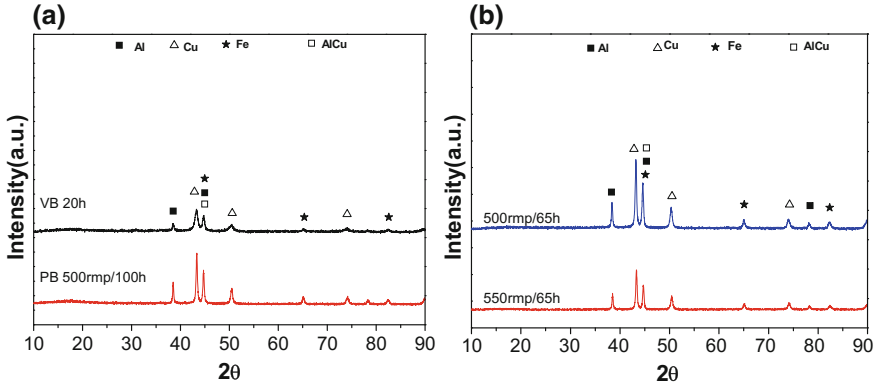

Fig. 1 **a** XRD patterns of $Al_{64}Cu_{23.5}Fe_{12.5}$ with different apparatus, planetary ball milling (PB), high-energy vibration ball milling (VB). **b** XRD patterns of the $Al_{64}Cu_{23.5}Fe_{12.5}$ powders under different rotation speed with planetary ball milling

promote the alloy formation of MA. But in line with the situation in Fig. 1b, it achieve part of the alloying.

Change of phase structure during MA. Figure 2a show XRD patterns of the as-milled $Al_{64}Cu_{23.5}Fe_{12.5}$ powder with various time intervals. The diffraction peaks obviously tend to broaden with increasing milling time, indicating the reduction of the powder size,and there no new phase was formed, but the peak of elemental aluminum, copper and iron decreased continuously. The XRD pattern reveals that the as-milled product after 65 h of MA consists of a new λ-Al(Cu, Fe) phase, β-Al(Cu, Fe) and the residual Al Fe and Cu. Since there is almost no interdiffusion between Cu and Fe [8], it is assumed that Al, Cu, Fe form a stable intermetallic compound AlCu and AlFe phase during the initial reaction. As the rest of the reaction progresses into the two phases, the Fe solid solution enters the AlCu phase or Cu enters the AlFe phase. During this process, the β phase and the γ phase play a transitional role as intermediate products, after which the AlCuFe alloy And doped some of the simple substance. In the experiment of this figure, perhaps because the speed is too high, the stress in the reaction process inhibits the reaction of the mesophase to the alloy phase, which hinders the solution reaction and quasi-crystal formation.

During the process for the production of lithium battery negative slurry with samples of different milling time, The magnetic stick was used. We found that the sample with short milling glue on the surface of magnetic stick. The sample with longer milling time did not show this phenomenon. This means that magnetic elemental Fe disappar during MA process. This is in accord with the XRD results (Fig. 2a). The diffraction peak of Fe gradually weakened with longer milling time. Magnetic measurements were performed on the AlCuFe powder with different milling time. The results are shown Fig. 2b. Curve *a* is milling 0 h samples, curves

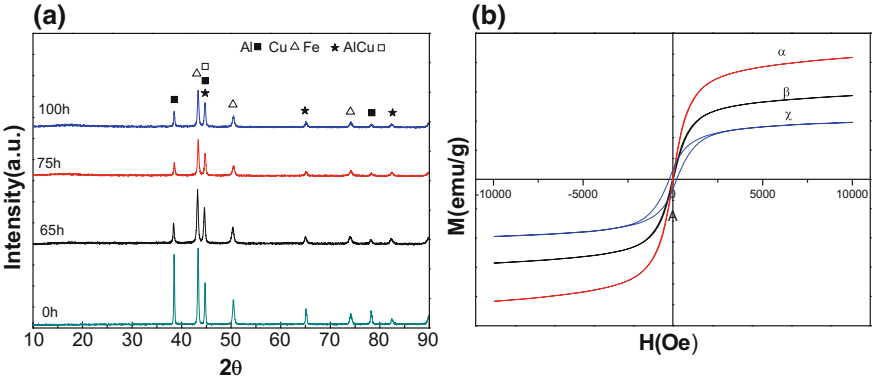

Fig. 2 **a** XRD patterns of the $Al_{64}Cu_{23.5}Fe_{12.5}$ powders with various MA time. **b** Magnetic property of $Al_{64}Cu_{23.5}Fe_{12.5}$ poeders after various MA times (α 0 h, β 10 h, χ 20 h)

b, *c* were samples milling 65, 100 h. With the increase of the milling time, the magnetism of the samples are getting weaker, indicating that the content of elemental Fe is gradually reduced during the process of milling. Fe element is dissolved in the other phase with the increase of the milling time, which leads to the weakness of the magnetism of samples. At this stage, part of the Fe element solid solution into the AlCu phase and the formation of AlCuFe alloy, the remainder is a mixture of Al, Cu, Fe powder and λ-Al_3Fe.

Electrochemical properties of $Al_{64}Cu_{23.5}Fe_{12.5}$ prepared by MA. A mixed powder of MA 100 h AlCuFe alloy [Al, Cu, Fe, λ-Al_3Fe, β-Al(Cu, Fe), AlCuFe] was prepared into a negative electrode sheet of a lithium ion battery and assembled into a lithium ion battery, followed by charge and discharge and a series of tests.

Figure 3a show the cycle-discharge specific capacity of AlCuFe alloy with different milling time. The first discharge capacity of the sample milling 100 h is 305 mAh g^{-1}, and the capacity is reduced to 190 mAh g^{-1} after 30 cycles. Milling 75 h samples also have similar circulatory trends, but it decays to a stable value of 180 mAh g^{-1} after 20 cycles. It can be seen that as the milling time of the sample increases, the discharge capacity of the sample increases.

Figure 3b shows the discharge capacity-cycle number of AlCuFe and pure Al. It can be seen that the first discharge capacity of pure Al is much larger, but its attenuation is extremely serious. After 20 cycle, the discharge capacity is almost zero. The samples of AlCuFe with 100 h milling were basically stable after 10 cycles, and the stable specific capacity reached 250 mAh g^{-1}, which was much higher than that of pure Al.

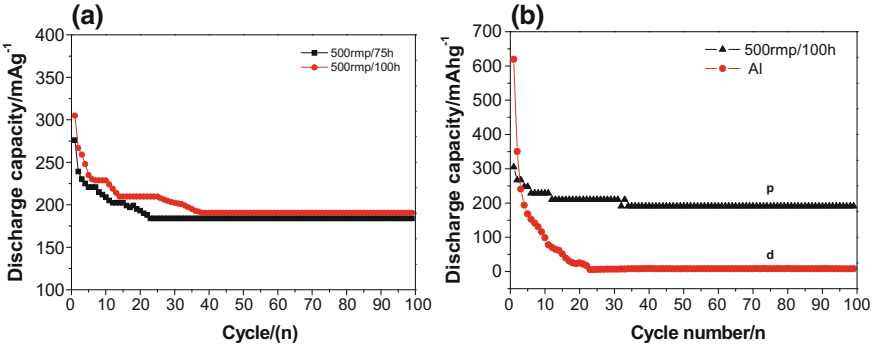

Fig. 3 **a** Cycling performance of different MA times. **b** Cycling performance of planetary ball mill 500 rmp MA 100 h (p) and pure Al (d) electrodes

Conclusion

In this paper, $Al_{64}Cu_{23.5}Fe_{12.5}$ was prepared by mechanical alloying using pure Al, Cu and Fe powder as the starting materials.

1. Changing the laboratory equipment, changing the milling time and speed can not achieve AlCuFe powder completely alloying. It is found that the fully alloyed of AlCuFe powder does not form directly from the milling process for a nominal composition of $Al_{64}Cu_{23.5}Fe_{12.5}$ powders, and a longer time milling results in the formation of part of alloying of AlCuFe after the MA treatment.
2. Under the condition of 500 rmp, the ferromagnetism of the material decreases with the increase of the milling time, and the peak value of the iron phase is greatly weakened, which indicates that the iron element may enter the other phase through solid solution.
3. The first specific discharge capacities are 308 and 278 mAh g^{-1} for 100, 75 h MA electrodes. With the increase of milling time and speed, the discharge capacity of lithium ion battery is obviously increased, and the stability is better. The optimised AlCuFe electrode shows improved lithium storage properties, outstanding cycling stability (198 mAh g^{-1} after 100 cycles). Compared with the negative electrode Al, AlCuFe alloy material has better stability, and the cycle performance, meanwhile the stability of the discharge capacity is higher.

Acknowledgements Project supported by Natural Science Foundation of Tianjin, No. 16JCTPJC51900.

References

1. S. Zheng, W. Yang, Y. Zhu, H. Zhou, J. Wang, J. Yang, In situ reduction and intercalation of graphite oxides for Li-S battery cathodes. J. Adv. Energy Mater. **1400482**, 5–9 (2014)
2. P.G. Bruce, B. Scrosati, J.-M. Tarascon, Nanomaterials for rechargeable lithium batteries. Angew. Chem. Int. Ed. **47**, 2930–2946 (2008)
3. M. Cao, M. Zhang, L. Xing, Q. Wang, X.-Y. Xue, One-step preparation of pomegranate-shaped Sn/SnO_x/nanocarbon composites for fabricating ultrafast-charging/long-life lithium-ion battery. J. Alloy. Compd. **694**, 30–39 (2017)
4. H. Liu, R. Hu, C. Huang, W. Sun, H. Zhang, M. Zhu, Toward cyclic durable core/shell nanostructure of Sn-C composite anodes for stable lithium storage by simulating its lithiation-induced internal strain. J. Alloy. Compd. **704**, 348–358 (2017)
5. R. Liu, W. Su, P. He, C. Shen, C. Zhang, F. Su, C.-A. Wang, Synthesis of SnO_2/Sn hybrid hollow spheres as high performance anode materials for lithium ion battery. J. Alloy. Compd. **688**, 908–913 (2016)
6. M. Mitka et al., Microstructure of mechanically alloyed and annealed $Al_{62}Cu_{25.5}Fe_{12.5}$ powder. J. Alloy. Compd. **653**, 47–53 (2015)
7. W. Yan, T. Ying et al., On phase transformations in mechanically alloyed and subsequently annealed $Al_{70}Cu_{20}Fe_{10}$. J. Intermetallics **16**, 121–129 (2008)
8. A.I. Salimon, A.M. Korsunsky, E.V. Shelekhov, T.A. Sviridova, S.D. Kaloshkin, V.S. Tcherdyntsev et al., Acta Mater. **49**, 1821–1833 (2001)